Temperature variations in the low stratosphere (50–200 hPa) monitored by means of the atmospheric muon flux

M. Aglietta[1][2], B. Alessandro[2], P. Antonioli[3], F. Arneodo[4],
L. Bergamasco[2][5], M. E. Bertaina[2][5][*], L. Briatore[5],
A. Castellina[1][2], A. Chiavassa[2][5], B. D'Ettorre Piazzoli[6],
G. Di Sciascio[6], S. Ferrarese[5], W. Fulgione[1][2], P. Galeotti[2][5],
P. L. Ghia[1][4], M. Iacovacci[6], A. Longhetto[5], M. Manfrin[5],
G. Mannocchi[1][2], C. Morello[1][2], G. Navarra[2][5], R. Richiardone[5],
O. Saavedra[2][5], A. Stamerra[5][**], G. C. Trinchero[1][2],
S. Valchierotti[5], P. Vallania[1][2], S. Vernetto[1][2] and C. Vigorito[2][5]

[1] *Istituto di Fisica dello Spazio Interplanetario - 10133 Torino, Italy*
[2] *INFN, Sezione di Torino - 10125 Torino, Italy*
[3] *INFN, Sezione di Bologna - 40126 Bologna, Italy*
[4] *INFN, Laboratori Nazionali del Gran Sasso - 67010 Assergi (AQ), Italy*
[5] *Dipartimento di Fisica Generale dell'Università - 10125 Torino, Italy*
[6] *Dipartimento di Scienze Fisiche dell'Università and INFN - 80125 Napoli, Italy*

Summary. — The dependence of the muon flux on the atmospheric parameters (pressure and temperature) is a well-known effect since long time ago. We have correlated the muon flux recorded by the electromagnetic detector of EAS-TOP with the atmospheric temperature (up to few hPa level) monitored by the radio-soundings of the ITAV—Aeronautica Militare at Pratica di Mare (Rome). A significant effect has been observed when the muon flux is correlated with the atmospheric temperature in the region 50–200 hPa, as expected, since this is the region where the mesons of first generation are produced. The technique has been applied to two short periods of strong temperature variations in the low stratosphere, showing that the temporal pattern of the temperature is fairly well reproduced by the variations of the muon flux. The main results of this analysis are presented.

PACS 43.28.Vd – Measurement methods and instrumentation to determine or evaluate atmospheric parameters, winds, turbulence, temperature and pollutants in air.
PACS 92.60.Xg – Stratosphere/troposphere interactions.
PACS 95.55.Vj – Neutrino, muon, pion, and other elementary particle detectors; cosmic ray detectors.

(*) E-mail: bertaina@to.infn.it
(**) Now at: Dipartimento di Fisica dell'Università and INFN, 56010 Pisa, Italy.

175

1. – Introduction

The stratosphere is subject to thermal variations whose origin is related to dynamical factors connected with the atmospheric planetary circulation and its anomalies. Sudden stratospheric warmings are among the most significant and remarkable variations, at least from the connections they have with Rossby planetary waves [1]. Stratospheric phenomena are usually studied by means of radio-soundings or satellite measurements which are quite precise, although not providing a continuous monitoring of the atmosphere.

The muon flux at ground level follows a power law spectrum which is the convolution of different factors: the primary cosmic-ray spectrum (the injection spectrum), the properties (lifetime and interaction length) of the parent mesons (pions π and kaons K) whose decays originate the muon μ flux, and the lifetime of the μ component. While the variations on the primary cosmic rays are of solar (*i.e.* Forbush decreases, flares) or of extra-solar origin (*i.e.* sidereal anisotropies), the cascade in atmosphere of the meson and muon components depends on the atmospheric parameters. The atmospheric effects on the μ flux have been the object of different studies in the past, among others [2-5] and they have been mathematically treated and summarized by Dorman [6].

In the past, cosmic-ray physicists have always corrected the μ flux for the atmospheric effects in order to study the primary cosmic-ray variations, however, the atmospheric μ flux could, conversely, be used as a probe of the atmospheric parameters, in particular of the temperature in the low stratosphere. This idea was already proposed in the past by Dorman [7] and applied by [8]. The peculiarities of this technique are: a) the possibility of performing an almost continuous monitoring of the atmospheric conditions (temperature data every two hours as it was experimentally determined); b) use of instruments already employed for other purposes in different locations of the planet.

In this paper we will study more in detail the method by correlating the muon counting rate measured by EAS-TOP [9] with the atmospheric temperature data provided by ITAV—Aeronautica Militare at Pratica di Mare (Rome). The method is applied to two particular periods of strong temperature variations in the low stratosphere and the results are presented. Finally, a more detailed analysis of these results has been conducted by taking into account the temperature and geopotential data of the same periods provided by the European Center for Medium range Weather Forecast (ECMWF). The cosmic-ray flux is monitored by means of the Neutron Monitor data of Rome [10], whose counting rate has a very weak dependence on the variations of the atmospheric temperature.

2. – The intercorrelation between atmospheric parameters and muon flux

The variation of the μ flux (C) related to the variation of atmospheric parameters can be parametrized by the following expression [6]:

$$(1) \qquad \frac{\delta C}{C} = k_p \delta h_0 + \int_0^{h_0} W_T(h) \delta T(h) \mathrm{d}h,$$

where k_p is the barometric coefficient, h_0 is the pressure at observation level and 0 the pressure at the top of the atmosphere, and $W_T(h)$ are the partial temperature coefficients that characterize the contribution of each atmospheric layer to the total temperature effect. While the barometric effect is always negative, the sign of the coefficients W_T depends on the threshold energy $(E_{\mu,\mathrm{thr}})$ of the detector. Experiments like EAS-TOP

TABLE I. – *Contribution of the upper layers (h < 250 hPa) to the temperature coefficient. Simulated data and experimental results are compared. The effect of the whole atmosphere is taken into account in the experimental result of BAKSAN.*

Experiment	$E_{\mu,\text{thr}}$	k_T (K^{-1}) $\times 10^4$ (sim.)	k_T (K^{-1}) $\times 10^4$ (exp.)
BAKSAN	220 GeV	25 ± 6	37.2 ± 3.8
EAS-TOP	3 MeV	-6.7 ± 1.3	-7.2 ± 1.5

with threshold energies in the MeV region [2] observe negative $W_T(h)$ coefficients because the effect is related to the surviving probability of the low energy muons from the production to the detection level[1]. On the other hand, experiments with $E_{\mu,\text{thr}}$ in the GeV [3, 4] or TeV [5] regions observe positive $W_T(h)$. In this case, the effect is related to the competitive processes of decay and interaction of the parent mesons π and K. Dorman's calculations show also that the predominant $W_T(h)$ coefficients are those related to the 50–200 hPa region, where muons are produced by the decay of the mesons of first generation. We have evaluated the extent of such contribution by means of an unidimensional simulation in which protons assumed as primary cosmic rays have been cascaded through an isothermal atmosphere. The temperature has then been changed only in the upper layers ($h < 250$ hPa) and the μ flux at ground level has been studied for different muon energy thresholds. Equation (1) has been simplified into the following relation where k_T is a coefficient that replaces $W_T(h)$ for the 50–200 hPa region, the barometric effect is expressed by means of the more intuitive variable P for pressure, and the finite increments are considered for the relative variation of the counting rate, and the absolute variation of pressure and temperature from reference values:

$$(2) \qquad \frac{\Delta C}{C} = k_p \cdot \Delta P + k_T \cdot \Delta T.$$

The results of the simulation and the experimental results of BAKSAN [4] and EAS-TOP are reported in table I. The sign and the magnitude of the two k_T experimental coefficients confirm the theoretical motivations and the fact that the low stratosphere provides the most important contribution to the total effect. This is especially true in case of BAKSAN where the experimental result is obtained taking into account the contribution of the entire atmosphere.

A remark has to be done here. Due to the completely different statistics involved in experiments with MeV or GeV $E_{\mu,\text{thr}}$ (muon counting rate $R_\mu \sim 10$ Hz for BAKSAN and ~ 3000 Hz/station in EAS-TOP), experiments with MeV thresholds are in principle sensitive to daily variations of the atmospheric temperature: $\sigma(\Delta T) = \frac{1}{|k_T|} \cdot \sqrt{\frac{2}{R_\mu \cdot \Delta t}} \sim 0.5$ K with $\Delta t = 2$ h as in the EAS-TOP case. On the other hand, in the experiment of BAKSAN, where $E_{\mu,\text{thr}}$ is in the hundred GeV region, a theoretical sensitivity of $\sigma(\Delta T) \sim 0.5$ K would require ~ 1.5 days of integration time, therefore underground detectors are only sensitive to seasonal variations (and in fact a seasonal variation of the average atmospheric temperature has been observed by BAKSAN and MACRO experiments [4, 5]).

---

[1] The energy threshold on the primaries is set by the geomagnetic rigidity, which is also the case for the primaries whose cascades generate the muons detected by EAS-TOP.

TABLE II. – *Barometric and temperature coefficients obtained for EAS-TOP in the three considered periods. The last column reports the temperature coefficients when the correction for the Neutron Monitor data is applied. The aveage value of the linear-correlation coefficient for the barometric effect in one station is $r \sim 0.9$ for all the periods. The average linear-correlation coefficient of the temperature effect in one station is reported inside the table (r_m values). The linear-correlation coefficents become more significant when the correction for the cosmic-ray variations is applied.*

Period	$k_p \times 10^3$ (hPa^{-1})	$k_T \times 10^4$ (K^{-1})	r_m	$k_T \times 10^4$ (K^{-1})	r_m-NM
A: 01/05/93-03/06/93	-3.89 ± 0.08	-9.6 ± 1.1	0.25	-9.5 ± 2.1	0.45
B: 11/02/93-15/03/93	-3.96 ± 0.07	-6.3 ± 2.2	0.26	-7.6 ± 2.2	0.44
C: 27/11/92-15/12/92	-3.43 ± 0.05	-2.6 ± 2.1	0.08	-4.5 ± 2.1	0.24

3. – Instruments and detectors

The analysis has been performed by correlating the atmospheric μ flux detected by the ElectroMagnetic Detector (EMD) of EAS-TOP [9] at Gran Sasso National Laboratory (LNGS) (42.27 °N, 13.34 °E) with the atmospheric temperatures measured by the radio soundings of Aeronautica Militare at Pratica di Mare (Rome). The data of the Neutron Monitor in Rome have also been used to correct for variations on the primary cosmic-ray flux. The two sites where cosmic rays were recorded were located at relative distances smaller than 100 km, justifying the assumption that at high altitudes the atmospheric conditions were similar. The cosmic-ray intensity and temperature measurements used in this analysis cover the period November 1992-July 1993.

The EMD detector at the time of these measurements was an array of 29 stations (10 m^2 each) of plastic scintillators (NE102A, 4 cm thick). Each station was divided into 16 scintillator units (80 cm × 80 cm each), each unit being viewed by a Philips XP3462B photomultiplier. Photomultiplier signals were discriminated at 0.3 m.i.p. threshold level ($E_{\mu,\mathrm{thr}} = 3$ MeV) and counted on a scaler. The array was covering an area of 500×300 m^2 at an atmospheric depth of 810 hPa, being sensitive to the charged component of the cosmic radiation (mainly μ). The typical μ counting rate of EMD was ~ 3 kHz/station. Each EMD station provided the μ counting rate every 100 s together with the local atmospheric pressure and temperature.

The radio-soundings were operated by Aeronautica Militare 2–4 times/day at 00, 06, 12 and 18 h UTC from the Pratica di Mare Station (41.66 °N, 12.45 °E) by launching Vaisala probes, model RS 80. The radio-soundings were providing different information, among others the temperature at several atmospheric layers. Levels were measured every few hPa, till 3 hPa height, with 0.1 hPa resolution and ±0.2 hPa accuracy. Temperature was obtained with 0.1 °C resolution and ±0.2 °C accuracy.

The Neutron Monitor in Rome [10] (41.90 °N, 12.52 °E) is a standard NM-64 type with 18 proportional counters divided in 3 detectors with 6 counters each. Further characteristics are ~ 6.2 GV vertical effective cut-off rigidity and ~ 150 Hz counting rate.

4. – Measurement of the temperature effect for EAS-TOP

Three periods were selected to be used in the present analysis (see table II). The technique was optimized on period A (see fig. 1) and then repeated in periods B and C
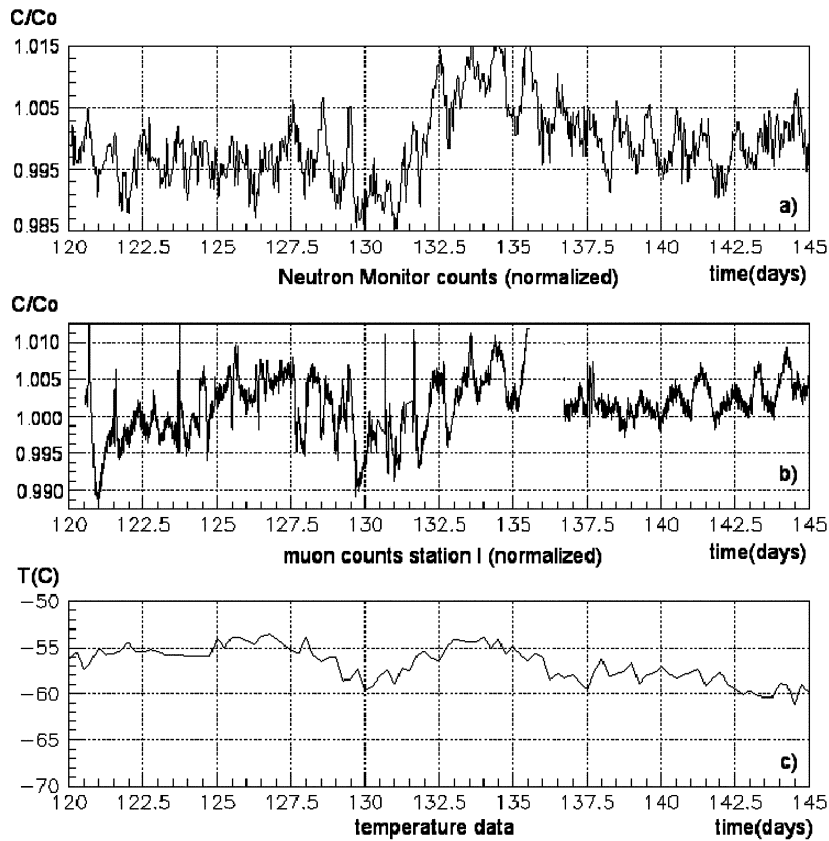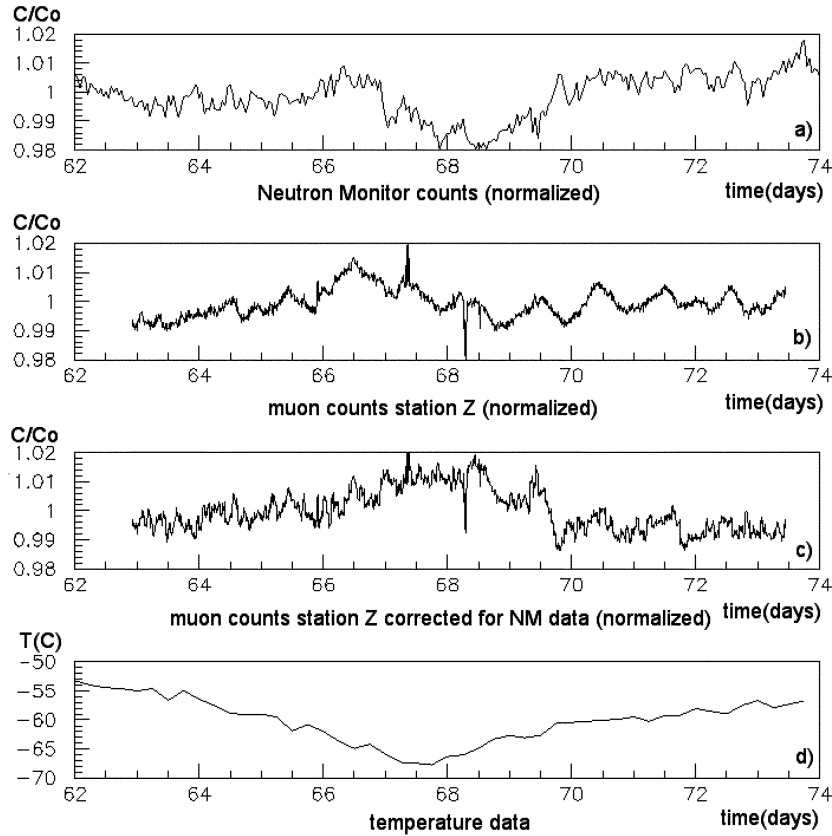
Fig. 1. – a) Hourly counting rate registered by the Neutron Monitor in Rome corrected for the barometric effect. b) Counting rate, every 10 minutes, of a EMD station corrected for the barometric effect. c) Average temperature in the 50–200 hPa region as recorded by the radio-soundings every 6 hours. Data refer to period A (see table II).

(see figs. 2 and 3), when particularly intense temperature variations in the low strato-sphere were recorded. In the analysis each EMD station is considered independent of the others and the effect is searched by looking at a similar response by several stations. First of all, the stability of the detector was studied. The data of each station showed a Pois-sonian behavior on a 100 s time scale (relative dispersion of the counting rate in different stations was $\sigma_{100s}/N_{100s} = (1.6\text{–}2.9) \times 10^{-2}\%$). The relative dispersion of the counting rate on a daily and monthly scale was $\sigma_{\mathrm{d}}/N_{\mathrm{d}} = 0.5\%$ and $\sigma_{\mathrm{m}}/N_{\mathrm{m}} < 1\%$, respectively.

The relative variations of the counting rate as a function of pressure and temperature have been searched according to eq. (2), applying two separated steps. In the first step, the barometric effect (k_p) is obtained as it is one order of magnitude higher (see table II). For this purpose an average counting rate ($\overline{C}$) and pressure ($\overline{p}$) are calculated every run (average duration about one week). Then, through a linear regression between the relative variation of counting rate (C) and pressure (p) measured every 10 minutes ($\frac{C-\overline{C}}{\overline{C}} = k_p \cdot (p - \overline{p})$), the coefficient k_p is extracted. Finally, the original counting rates, renormalized for the barometric effect, are averaged in intervals of two hours around the temperature data (C^p).

Fig. 2. – a) Hourly counting rate registered by the Neutron Monitor in Rome corrected for the barometric effect. b) Counting rate, every 10 minutes, of a EMD station corrected only for the barometric effect, and c) hourly counting rate corrected also for the neutron monitor data. d) Average temperature in the 50–200 hPa region as recorded by the radio-soundings every 6 hours. Data refer to period B (see table II).

In the following step the temperature effect is obtained. The temperature (T) used in this correlation is the average value between the three temperatures T_{50}, T_{100} and T_{200} given by the radio-soundings at the 50 hPa, 100 hPa, and 200 hPa levels. This selection was decided after a study performed on the dependence of k_T on the temperature used in the correlation, choosing different values and combinations of temperature values of the layer 50–300 hPa, which showed that the most significant effect was obtained by averaging the three temperatures at 50 hPa, 100 hPa and 200 hPa. The coefficient k_T is extracted from a fit to the variation of the relative counting rate as a function of the temperature variation in consecutive radio-soundings i: $(T_{i+1} - T_i; \frac{C^p_{i+1}-C^p_i}{C^p_i})$—see fig. 4. Figure 4 shows an example of $\frac{\Delta C}{C}$ vs. ΔT for 2 stations in period A, while on the bottom of the same figure, the distribution of 23 k_T values (corresponding to 23 different stations), during the same period, is shown. The coefficients of all the stations are negative and of the same magnitude—$K_T = (-9.6 \pm 5.3) \times 10^{-4} \, \mathrm{K}^{-1}$—indicating that the whole array was measuring the same effect. Several checks have been performed in order to verify that the effect was related to the temperature in the low stratosphere (see table III).
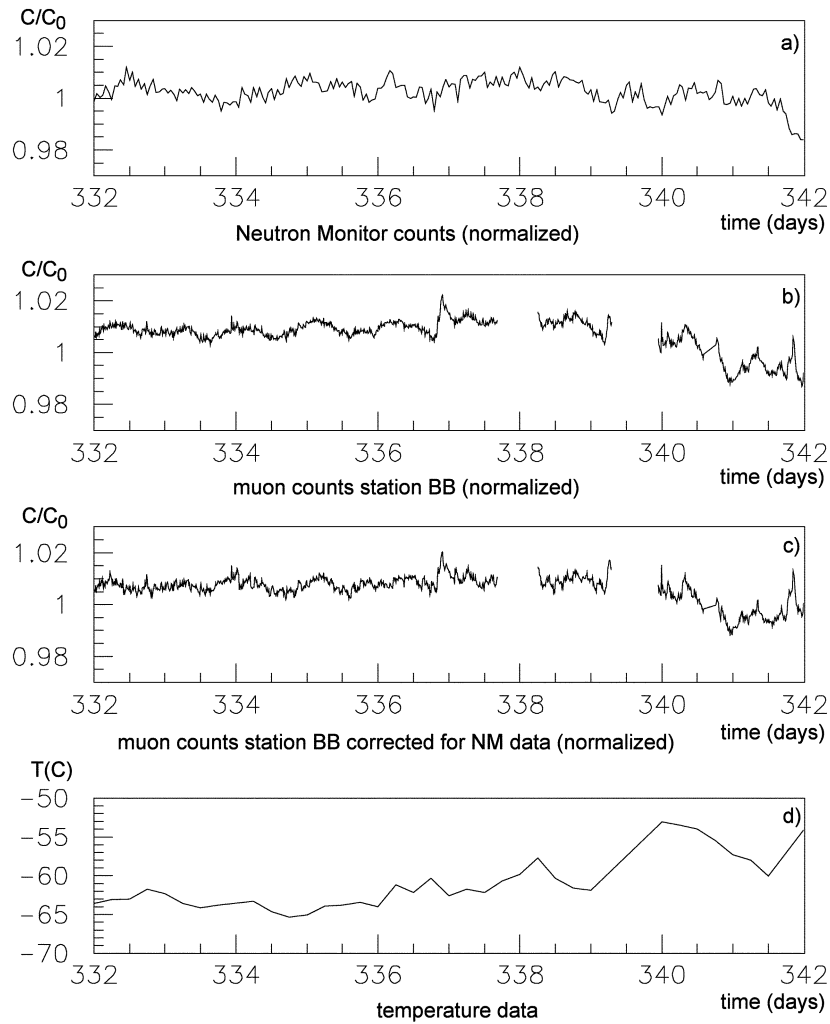
Fig. 3. – a) Hourly counting rate registered by the Neutron Monitor in Rome corrected for the barometric effect. b) Counting rate, every 10 minutes, of a EMD station corrected only for the barometric effect, and c) hourly counting rate corrected also for the neutron monitor data. d) Average temperature in the 50–200 hPa region as recorded by the radio-soundings every 6 hours. Data refer to period C (see table II).

No significant dependence was obtained by correlating $\frac{\Delta C}{C}$ with the local temperature (T_{loc}), and no significant correlation was found between the local pressure (p) and the temperature in low stratosphere (T_{100}), except for some slight ones observed in period C (as described more in detail in the next section, period C shows a more complex situation from the atmospheric point of view compared to A and B). No residual pressure effects were found. A ± 6 h shift was applied to the T_{100} values and the correlation almost disappeared: $k_T(-6\,\text{h}) = (2.3 \pm 1.4) \times 10^{-4}\,\text{K}^{-1}$, $k_T(+6\,\text{h}) = (-1.3 \pm 1.4) \times 10^{-4}\,\text{K}^{-1}$.

In order to verify that the dependence was not related to the primary cosmic-ray flux, the μ data, renormalized by the barometric effect, were corrected for the neutron
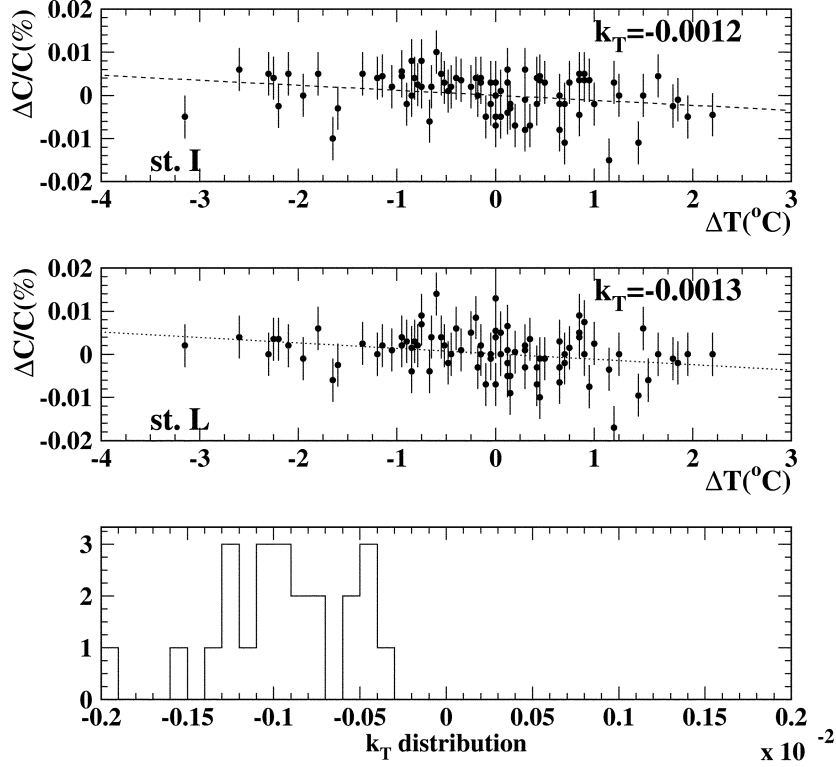
Fig. 4. – Relative counting rate variation $\frac{\Delta C}{C}$ *vs.* ΔT for 2 stations in period A in the top part of the figure, while the distribution of the 23 k_T values, during the same period, is shown in the bottom part. The μ counting rate is obtained integrating two hours of data around the temperature data.

monitor data, and only after this correction, the temperature effect was searched. Results are shown in the last column of table II, and indicate that the temperature coefficient becomes even more significant in periods B and C, and unchanged in period A. Finally, the k_T values are of the same magnitude as expected (see table I). The differences among the three values have to be ascribed to the influence of other physical effects (*i.e.* contribution of the tropospheric levels, decoupling of temperature and geopotential variations) as discussed in sect. **5**.

TABLE III. – *Various attempted correlations. Only for period C some correlations are significant. See text for details.*

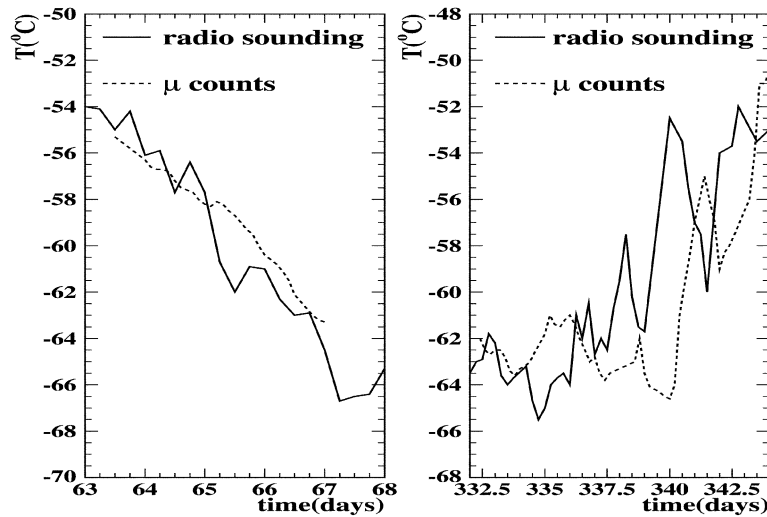| Measurement	Technique	Coefficient	Period A	Period B	Period C
Pres. residual effects	$\frac{\Delta C}{C}$ *vs.* ΔP_{res}	k_p $(\text{hPa}^{-1}) \times 10^4$	2.3 ± 1.0	2.0 ± 1.0	-0.2 ± 0.5
Pres. *vs.* stratos. T	Δp_{800} *vs.* ΔT_{100}	k_{pT} (hPa/K)	0.0 ± 0.1	-0.1 ± 0.2	-0.4 ± 0.1
Local T effects	$\frac{\Delta C}{C}$ *vs.* ΔT_{loc}	$k_{T\text{loc}}$ $(\text{K}^{-1}) \times 10^4$	1.3 ± 1.2	-2.4 ± 1.5	4.6 ± 0.9
Correl. T loc. and T stratos.	ΔT_{100} *vs.* ΔT_{loc}	k_{TT} (K/K)	0.2 ± 0.1	0.1 ± 0.1	0.0 ± 0.1

Fig. 5. – Original temporal behavior of the temperature in the low stratosphere (average of layers 50–200 hPa) and temporal pattern of the temperature as extracted from the variations of the μ counting rates at EAS-TOP. Left figure refers to period B and right figure to period C for one station (similar patterns are obtained for the other stations, not shown here). The μ counting rate is bi-hourly integrated, while temperature data are measured every 6 hours. A 6 h moving average is applied in the plot to the μ counting data to smear out short-time fluctuations.

5. – Monitoring temperature variations

The significant correlation between muon counting rates and temperature variations in the low stratosphere, suggested the possibility of following strong temperature variations in the low stratosphere by means of the muon flux. In periods B and C the upper atmosphere was characterized by sudden and significant temperature variations lasting ~ 1 week each. In the same period muon counting rates registered by the EMD stations showed a tendency for specular trends (see figs. 2 and 3). It is interesting to observe at this point that period A, which was a quiet period from the point of view of the temperature in the low stratosphere, does not show any specific trend in the μ flux too. Concerning the Neutron Monitor data, during period C no specific trend is observed, while in period B a significant variation of the flux was observed between days 67 and 70. For this reason, the analysis of period B was limited between days 63 and 67. It is interesting, however, to point out that after the correction with the Neutron Monitor data, the trend of the μ counting rates becomes specular to the stratospheric temperature also between days 67 and 70 (see fig. 2).

For a more quantitative analysis of the periods with significant temperature variations, after the correction for the barometric effect, the coefficient K_T was extracted from the following relationship:

$$(3) \qquad \frac{C^p - \overline{C^p}}{\overline{C^p}} = K_T \cdot (T - \overline{T}),$$

where $\overline{C^p}$ and $\overline{T}$ represent the average counting rate and temperature in the period of
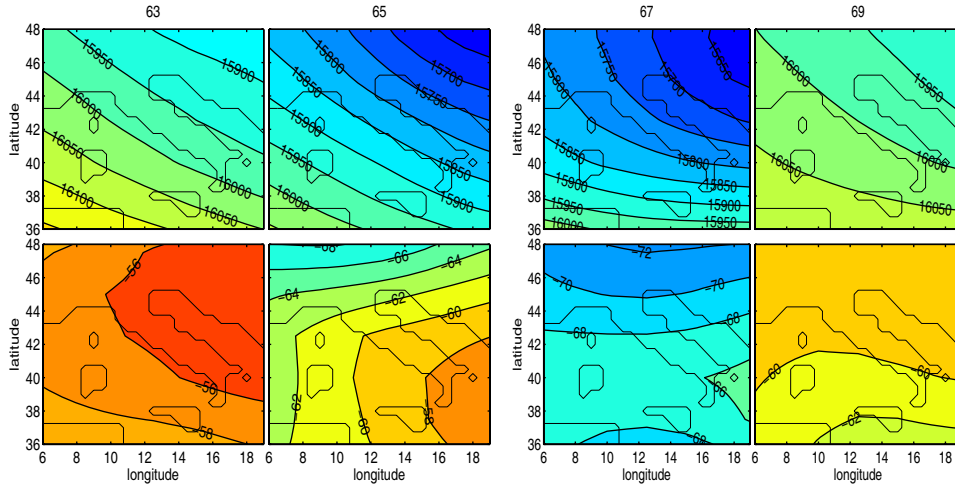
Fig. 6. – Geopotential heights (m)—top—and temperatures (°C)—bottom—at 100 hPa level for period B in 4 different days (63, 65, 67, 69) as obtained from ECMWF.

analysis (see fig. 5). By inverting such relationship

$$(4) \qquad\qquad T_\mu = \frac{1}{K_T} \cdot \frac{C^p - \overline{C^p}}{\overline{C^p}} + \overline{T}\,,$$

we can estimate how well the muon flux is able to reproduce the temporal behavior of the temperature in the stratosphere (T_μ). Figure 5 shows that the general trend of the temperature in the selected part of period B is clearly reproduced by the muon flux. The same technique applied also to period C shows a similar trend.
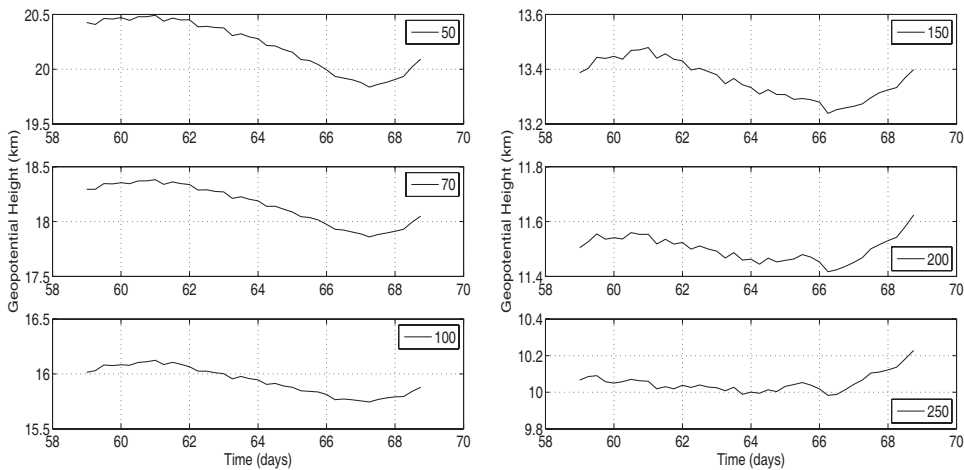
Fig. 7. – Temporal behavior of geopotential height at different atmospheric levels (hPa in the legend) for period B (data obtained every 6 hours).
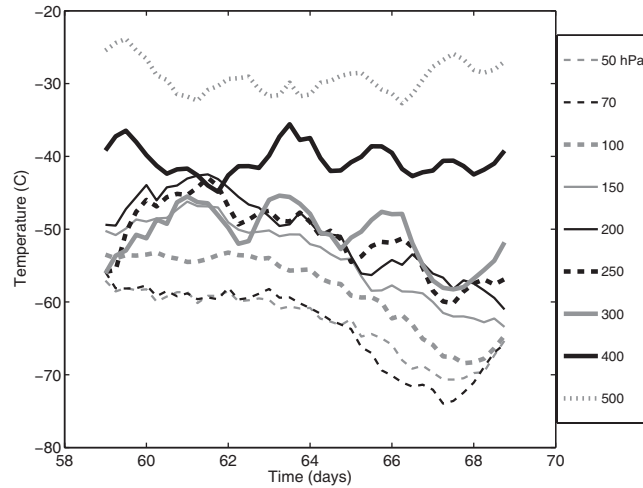
Fig. 8. – Temporal behavior of the atmospheric temperature at different atmospheric levels for period B (data obtained every 6 hours).

A more detailed analysis of the two periods shown in fig. 5 has been conducted by taking into account temperature and geopotential data of the same periods from ECMWF. While the data from ITAV provide point-like information on the Rome-Gran Sasso area, the ECMWF data allow a synoptic view on a much wider scale. Figure 6 shows the temporal behavior of the geopotential height and temperature at the atmospheric level of 100 hPa for 4 different days (63, 65, 67 and 69) of period B, while figs. 7 and 8 show the geopotential and temperatures at different atmospheric levels for the same period. All the levels between 50 and 200 hPa show the same trend for the geopotential, this applies also for the temperature data. The temperature measured through the μ counting rate follows the trend of the temperatures at the 50–200 hPa levels in conformity
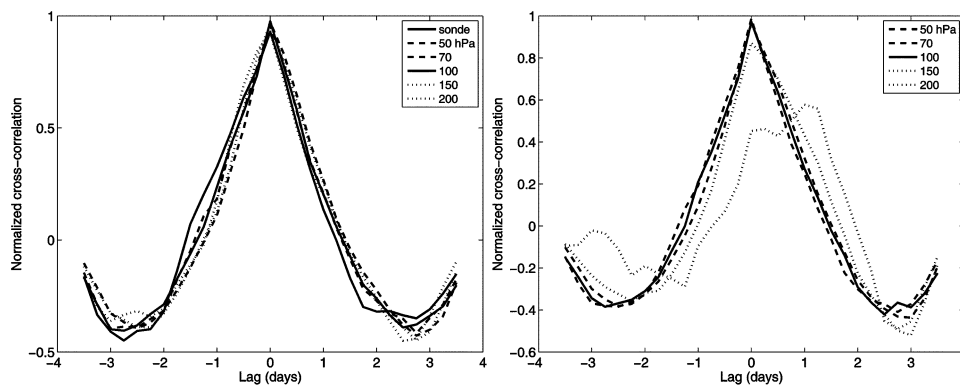

Fig. 9. – Cross-correlation study between the temperature extracted from the muon counts and the temperature from radio-soundings (average of the 50–200 hPa levels, see text), and from ECMWF for the 50–200 hPa atmospheric layers in period B (left). Same cross-correlation study between geopotential and temperature from ECMWF (right). Data are obtained every 6 hours.
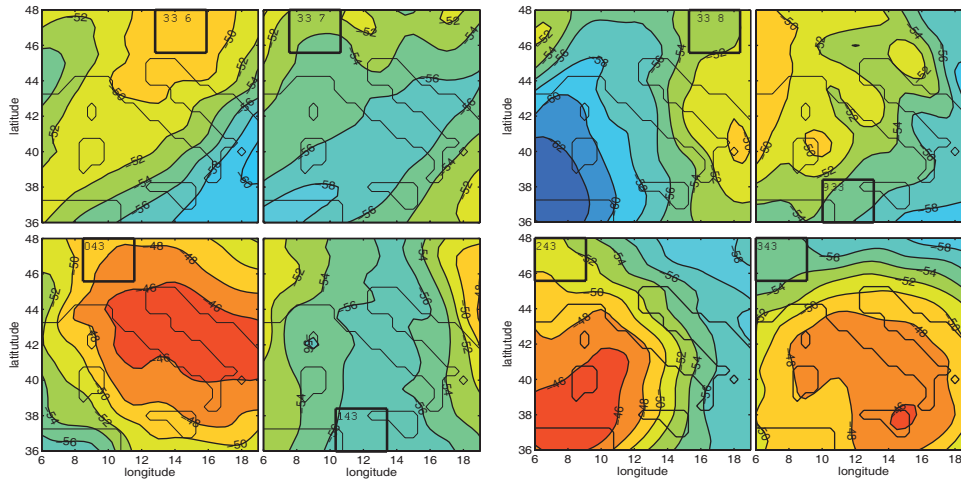
Fig. 10. – Temperatures (°C) at 200 hPa level for period C in 8 consecutive days (336–343) as obtained from ECMWF.

with the expectations. The good correlation between the temperatures extracted from the muon counts and the temperatures of the stratospheric layers is confirmed by their cross-correlation study shown in fig. 9. A sharp peak centered around lag time 0 days is observed for all the stratospheric layers. This is also valid for the cross-correlation study between temperatures and geopotentials, indicating that geopotential and temperature are well correlated at all levels, moreover, the low stratosphere behaves in a homogeneous way. Finally, it should be noticed from figs. 7 and 8 that the mid levels of the troposphere (400–500 hPa) show a different behavior (almost constant temperature in the whole period). This is another indication that the major contribution to the temperature effect comes from the low stratospheric levels.

Concerning period C, a closer look to fig. 5 shows, however, a more variable situation. The general trend between the temperature extracted from the muon counts and the temperature from the radio-soundings is similar, however, the temperature fluctuations are higher, and some delay (~ 1 day) between the two series of data is present. Figure 10 shows the temporal behavior of the geopotential and temperature at the atmospheric level of 200 hPa for 8 different days (336–343). Alternating days of warm and cold pulses are observed. This situation is present at different atmospheric levels (see fig. 11). A similar, unstable, situation is observed also on the geopotential trend (see fig. 12). Moreover, the temporal behavior of the geopotential and of the temperature is different among the atmospheric levels. While temperatures at levels above 250 hPa show an increasing trend, the lower levels behave in an opposite way. The strong warm pulse on the 250–200 hPa surface around day 341 has to be underlined. This pulse is inverted around level 300 hPa and vanishes progressively while moving towards upper levels. The behavior of the geopotential is at the same level opposite: in the same day in which there is the temperature pulse, the geopotential shows a minimum. This dishomogeneous behavior of the different atmospheric levels is evident also in the cross-correlation studies performed for period C (see fig. 13). A cross-correlation peak between the temperatures of the ITAV sonde and that extracted from the muon counts is present at time lag -1 days. Same lag of ~ 1 day is present in the cross-correlation between ECMWF data
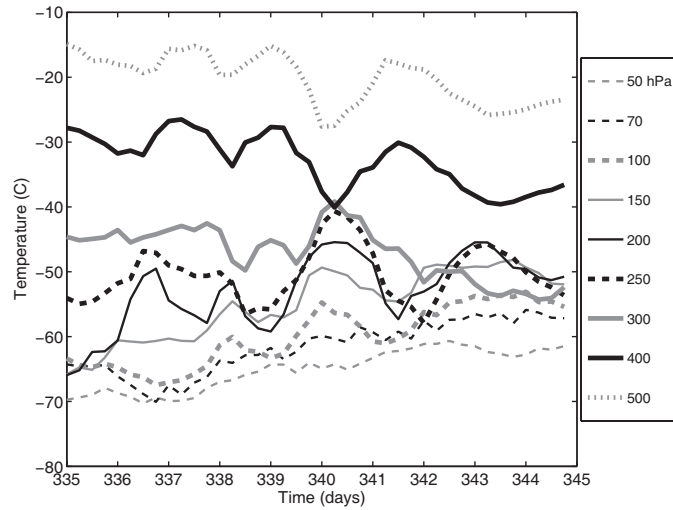
Fig. 11. – Temporal behavior of the atmospheric temperature at different atmospheric levels for period C. Data are obtained every 6 hours.

and temperatures extracted from the muon counts. The peak itself looks wider and less pronounced compared to period B. The cross-correlation study between temperatures and geopotential from ECMWF shows a different behavior for the different atmospheric levels, which clearly confirms the dishomogenous behavior of the low stratosphere in this period.
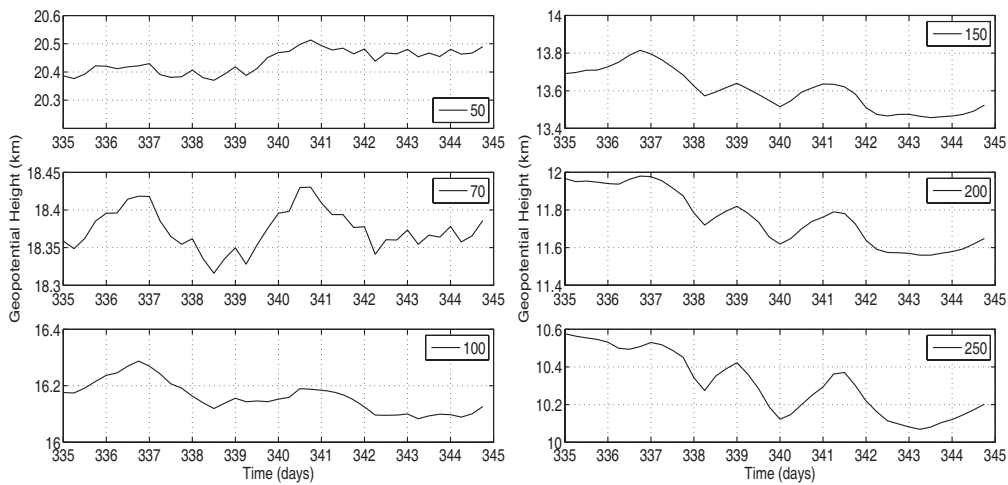

Fig. 12. – Temporal behavior of geopotential height at different atmospheric levels (hPa in the legend) for period C. Data are obtained every 6 hours.
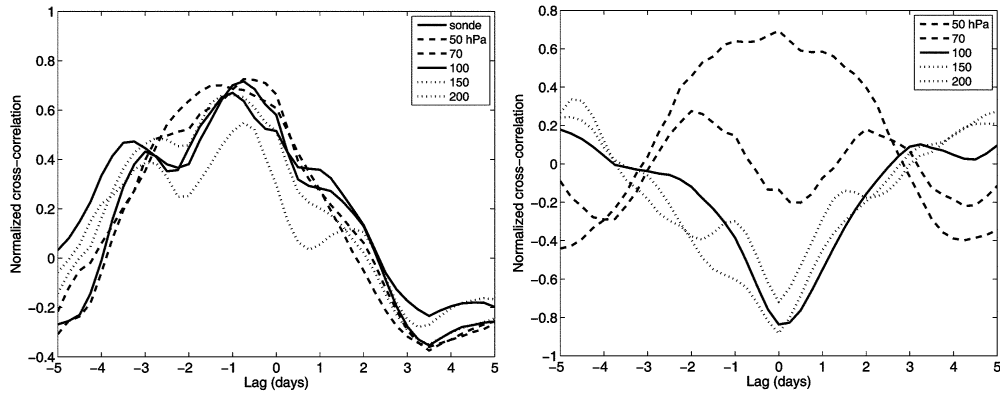
Fig. 13. – Cross-correlation study between the temperature extracted from the muon counts and the temperature from radio-soundings (average of the 50–200 hPa levels, see text), and from ECMWF for the 50–200 hPa atmospheric layers in period C (left). Same cross-correlation study between geopotential and temperature from ECMWF (right). Data are obtained every 6 hours.

6. – Conclusions

It has been shown that the EMD detector of EAS-TOP was sensitive to the temperature variations in the lower stratosphere. The results are in fair agreement with the expectations and confirm the significant role played by the 50–200 hPa levels to de-
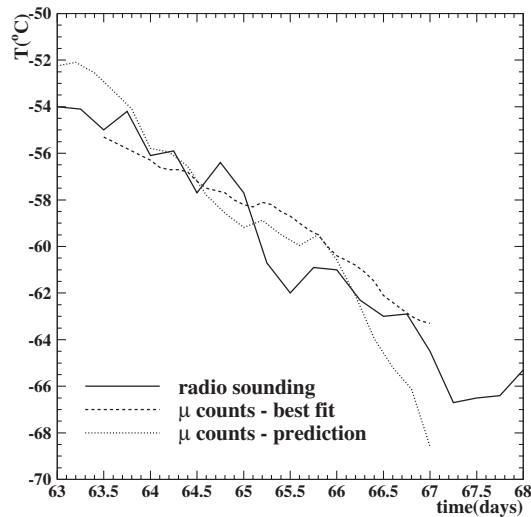

Fig. 14. – Temperatures predicted for period B by the μ counts (μ counts—prediction), compared with the original temporal behavior of the temperature in the low stratosphere (radio sounding), and the best temporal pattern of the temperature as extracted from the variations of the μ counting rates, as explained in sect. 5 (μ counts—best fit). The μ counting rate is bi-hourly integrated, while temperature data are measured every 6 hours. A 6 h moving average is applied in the plot to the μ counting data to smear out short-time fluctuations.

termine the temperature effect on the muon flux. Several checks on other observables strengthen this result. The technique is used to follow strong temperature variations in the 50–200 hPa region in a couple of cases. The muon counting rate at ground level follows the general trend of the temperature in both cases, and it is sensitive to sharp variations, such as those occurring during sudden warmings. Moreover, it is sensitive to the more or less homogenoeus behavior of the different atmospheric levels in the low stratosphere. Having the possibility of a continuous monitoring, this technique could thus integrate the more standard atmospheric data. In order to better quantify the intrinsic uncertainties of the muon technique to predict temperature variations in the low stratosphere, the sudden cooling of period B, which is our best example also from the atmospheric point of view for the considerations of sect. **5**, has been re-analyzed assuming only the knowledge of the average temperature of the period ($\overline{T}$)—see eq. (4). In this case a $K_T = -7.2 \times 10^{-4}\,\mathrm{K}^{-1}$ (average of the three k_T reported in the last column of table II) has been used. The results are presented in fig. 14 together with the temperatures measured by ITAV and by those extracted through the muon technique as explained in sect. **5**. As expected, the temporal pattern of the temperature in the period is fairly reproduced. The dispersion of the T_μ values around the true ones is on average $\sigma_{T_{\mu s}} \sim 1.7\,^\circ\mathrm{C}$ providing a quantitative estimation of the sensitivity of the muon technique as an independent probe of the temperature evolution in the low stratosphere, in simple atmospheric conditions. The sensitivity would surely worsen in less homogeneous atmospheric situations such as in period C.

We remind that muon detectors and neutron monitors are operating in different locations of the planet and, therefore, they could already provide data on a large scale.

$$* \; * \; *$$

REFERENCES

[1] Schoeberl M., *Rev. Geophys. Space Phys.*, **16** (1978) 521.
[2] Ekström L., *Ark. Geofys.*, **5** (1966) 129.
[3] Cini Castagnoli G. and Dodero M. A., *Nuovo Cimento B*, **51** (1967) 525.
[4] Andreyev Yu. M. *et al.*, *Proceedings of 21st ICRC, Adelaide*, Vol. **7** (1990), p. 88.
[5] Ambrosio M. *et al.* (MACRO Collaboration), *Phys. Rev. D*, **67** (2003) 042002.
[6] Dorman L., *Cosmic Ray Variations* (State Publishing House, Moskow) 1957.
[7] Dorman L., *Cosmic Ray Meteorological Effects* (Nauka, Moscow) 1972.
[8] Borog V. V. *et al.*, *Proceedings of 29th ICRC, Pune*, Vol. **2** (2005), p. 381.
[9] Aglietta M. *et al.* (EAS-TOP Collaboration), *Nucl. Instrum. Methods A*, **23** (1988) 277.
[10] Iucci N. *et al.*, *Nuovo Cimento C*, **7** (1984) 732.